Phospho-Profiling Linking Biology and Clinics in Pediatric Acute Myeloid Leukemia

Angela Schumich[1], Michaela Prchal-Murphy[2], Margarita Maurer-Granofszky[1], Andrea Hoelbl-Kovacic[2], Nora Mühlegger[1], Ulrike Pötschger[1], Sabine Fajmann[2], Oskar A. Haas[1], Karin Nebral[1], Nils von Neuhoff[3], Martin Zimmermann[4], Heidrun Boztug[5], Mareike Rasche[3], Marlies Dolezal[6], Christiane Walter[3], Dirk Reinhardt[3], Veronika Sexl[2], Michael N. Dworzak[1]

Correspondence: Michael N. Dworzak (e-mail: dworzak@stanna.at).

Abstract

Aberrant activation of key signaling-molecules is a hallmark of acute myeloid leukemia (AML) and may have prognostic and therapeutic implications. AML summarizes several disease entities with a variety of genetic subtypes. A comprehensive model spanning from signal activation patterns in major genetic subtypes of pediatric AML (pedAML) to outcome prediction and pre-clinical response to signaling inhibitors has not yet been provided. We established a high-throughput flow-cytometry based method to assess activation of hallmark phospho-proteins (phospho-flow) in 166 bone-marrow derived pedAML samples under basal and cytokine stimulated conditions. We correlated levels of activated phospho-proteins at diagnosis with relapse incidence in intermediate (IR) and high risk (HR) subtypes. In parallel, we screened a set of signaling inhibitors for their efficacy against primary AML blasts in a flow-cytometry based ex vivo cytotoxicity assay and validated the results in a murine xenograft model.

Certain phospho-signal patterns differ between genetic subtypes of pedAML. Some are consistently seen through all AML subtypes such as pSTAT5. In IR/HR subtypes high levels of GM-CSF stimulated pSTAT5 and low levels of unstimulated pJNK correlated with increased relapse risk overall. Combination of GM-CSF/pSTAT5^{high} and basal/pJNK^{low} separated three risk groups among IR/HR subtypes. Out of 10 tested signaling inhibitors, midostaurin most effectively affected AML blasts and simultaneously blocked phosphorylation of multiple proteins, including STAT5. In a mouse xenograft model of *KMT2A*-rearranged pedAML, midostaurin significantly prolonged disease latency. Our study demonstrates the applicability of phospho-flow for relapse-risk assessment in pedAML, whereas functional phenotype-driven ex vivo testing of signaling inhibitors may allow individualized therapy.

Introduction

Acute myeloid leukemia (AML) is a highly heterogeneous disease, the second most frequent leukemia entity in children and adolescents, and definitely the most aggressive variant. Despite continued progress and refinement of therapeutic approaches, about 35% of pediatric patients with the disease still suffer from relapse.[1,2] Constitutive activation of one or more signaling pathways in AML cells is associated with poor prognosis.[3] Hence, signal pathway interception in addition to current chemotherapy regimen has emerged as a novel approach for the treatment of adult as well as of pediatric AML.[4–6] Recently, midostaurin, a multitargeted kinase- and first generation FLT3-inhibitor, has been shown to significantly prolong overall and event-free survival among AML patients with a *FLT3* mutation in

combination with standard chemotherapy.[4] The application of signaling inhibitors in AML based solely on the presence of specific underlying genetic aberrations, such as *FLT3*-ITD or mutations in isocitrate dehydrogenase (*IDH)* may, however, represent a major limitation for their use since most signaling inhibitors- especially of first- and second generation- are by no means absolutely specific for a single target, but rather inhibit multiple kinases.[7] These 'off-target' effects could be therapeutically exploited in patients lacking the primary genetic target aberration. Accordingly, midostaurin shows activity not only in *FLT3*-mutated but also in *FLT3* non-mutated AML patients.[8] In a recent phase II open-label study in patients with relapsed AML the *FLT3*-ITD mutation status, albeit being predictive for response to AC220 (quizartinib), showed a high error rate as tool for stratification of patients into responders and non-responders.[9] Hence, there is a need for functional precision medicine moving beyond pure genomic target selection[10] to explain the heterogeneity of treatment response more accurately and to provide precise prognostic information for risk identification and to guide the use of targeted therapy. Phospho-signal profiling (phospho-flow) has the potential to be a powerful ally to current genomic approaches for prediction of relapse risk as well as of drug responses. Phospho-flow identified G-CSF induced pSTAT3 as predictive for survival in pedAML[11] and fedratinib (FED)- mediated reduction of pSTAT5 levels was identified as a predictive biomarker for *in vivo* drug-responses.[12] In a phosphoproteome analysis of primary AML blasts a signature consisting of 5 phosphorylation sites predicted the response of a small cohort of adult AML patients to AC220.[13] A comprehensive model spanning from signal activation patterns in the major genetic subtypes of pedAML to outcome prediction and to testing of signaling inhibitor effects in primary pedAML blasts has, however, not been provided so far. We therefore conducted a retrospective pilot study using phospho-flow based signal pattern profiling of primary bone marrow (BM) derived AML blasts from pedAML patients to determine whether phospho-flow can be used to (i) link distinct phospho-profiles to genetic subtypes of pedAML (ii) refine risk stratification in pedAML and (iii) predict or monitor response to signaling inhibitor treatment ex vivo.

Results

Flow-cytometry screen of phospho-profiles in AML under basal conditions

We measured intracellular levels of activated (phosphorylated) STAT1, STAT3, STAT5, NF-KB p65, AKT, S6, 4E-BP1, ERK1/2, p38 and JNK – signaling molecules which are fundamental to biologic processes in normal and leukemic hematopoiesis. A schematic overview of our gating strategy is provided in (Fig. 1A). We analysed a cryo-collection of primary BM derived cells of 166 pedAML patients (Fig. 1B). In the absence of any stimulation we detected activation for all assessed signaling molecules with strongest levels in p4E-BP1, pS6, and pSTAT5 overall (Fig. 1C and Suppl. Fig. 1A, Supplemental Digital Content, http://links.lww.com/HS/A52).

To reveal whether basal signal activation patterns differ between different genetic subtypes of pedAML, we stratified samples with conclusive genetic information (n = 132) according to seven relevant genetic subgroups.[14,15] As shown in Fig. 1D, we observed commonly higher basal activation levels in the *KMT2A*-rearranged (*KMT2Ar*) group compared to other genetic subsets in most signaling molecules except for pSTAT5, p4E-BP1, pp38,

and pJNK. A similar trend was apparent in the "other" as well as the *CBFB-MYH11* group with a lower intensity and consistency. Phospho-JNK was more frequently elevated in subtypes regarded as low risk (LR) pedAML. *RUNX1-RUNX1T1* and *PML-RARA* subsets exhibited an otherwise rather silent basal signaling profile.

Flow-cytometry screen of phospho-profiles in AML under ex-vivo cytokine stimulation

We exposed 166 primary patient samples to G-CSF, GM-CSF, Flt-3 ligand (FL), SCF, SDF, IL-3, TPO, IFNγ or a combination thereof ("cocktail") to measure ligand-induced phosphorylation ex vivo. Cytokine concentrations used corresponded to those found in serum of AML patients.[16–20] Basal signal activation levels (no cytokine stimulation, Fig. 1C-D) served as reference. In the "cocktail" setting, we detected prominent stimulation of pSTAT5, pAKT, pS6 and to a lesser extent of pERK1/2, p4E-BP1, and pSTAT3 (Fig. 2A). In the "cocktail plus" setting (including IFNγ) we additionally observed increased levels of pSTAT1 (Fig. 2A). Distinct cytokines elicited specific phospho-signal(s) (Fig. 2B), but p38, NF-KB and JNK were not further stimulated by any cytokine. As expected, G-CSF strongly engaged pSTAT3 and pSTAT5, IFNγ mostly pSTAT1 and pSTAT5. GM-CSF, IL-3 and TPO provoked predominantly pSTAT5. SCF, SDF, and FL primarily stimulated AKT, S6 and 4E-BP1 phosphorylation. Phospho-ERK1/2 rose mainly under FL stimulation and to a lesser extent with SCF and G-CSF. Altogether, the most pronounced changes were observed in levels of pSTAT5 which was activated by many cytokines (G-CSF, GM-CSF, IL-3, TPO and IFNγ).

Differences of cytokine-induced signal activation between different genetic subtypes of pedAML were also investigated (Fig. 2C). We excluded *GATA-1* patients due to restricted numbers. We found consistent increases in pSTAT5 upon G-CSF, GM-CSF, and IL-3 irrespective of the subtype. NK and *RUNX1-RUNX1T1* cohorts reacted with pSTAT5 also upon TPO stimulation. Elevated levels of pSTAT3 were seen in response to G-CSF throughout all subtypes, but with strongest stimulation among *RUNX1-RUNX1T1* and *PML-RARA* samples. More specifically, G-CSF showed its broadest effects in the *RUNX1-RUNX1T1* subset, where it stimulated also pAKT, pS6, p4E-BP1, and pERK1/2. These four signaling molecules were broadly stimulated through FL and SCF among *RUNX1-RUNX1T1* and *CBFB-MYH11* cases, whereas *PML-RARA* remained non-responsive. SDF activated pS6 and p4E-BP1 in *CBFB-MYH11* and *KMT2Ar* cases only. Single patient specific profiles are provided in Suppl. Fig. 1B (Supplemental Digital Content, http://links.lww.com/HS/A52).

Phospho-signal levels at diagnosis and risk of relapse

We retrospectively analyzed basal and cytokine induced phospho-signal levels in AML blasts from diagnosis and correlated them with the incidence of relapse.

Due to low numbers of relapses among LR cases (4 among 42) we focused on 90 intermediate / high risk (IR/HR) patients (41 relapses) (Suppl. Fig. 2A and B, Supplemental Digital Content, http://links.lww.com/HS/A52). We found that patients with and without a relapse showed differential activation of 13 signal nodes at diagnosis (Suppl. Fig. 2C, Supplemental Digital Content, http://links.lww.com/HS/A52). More specifically, patients who
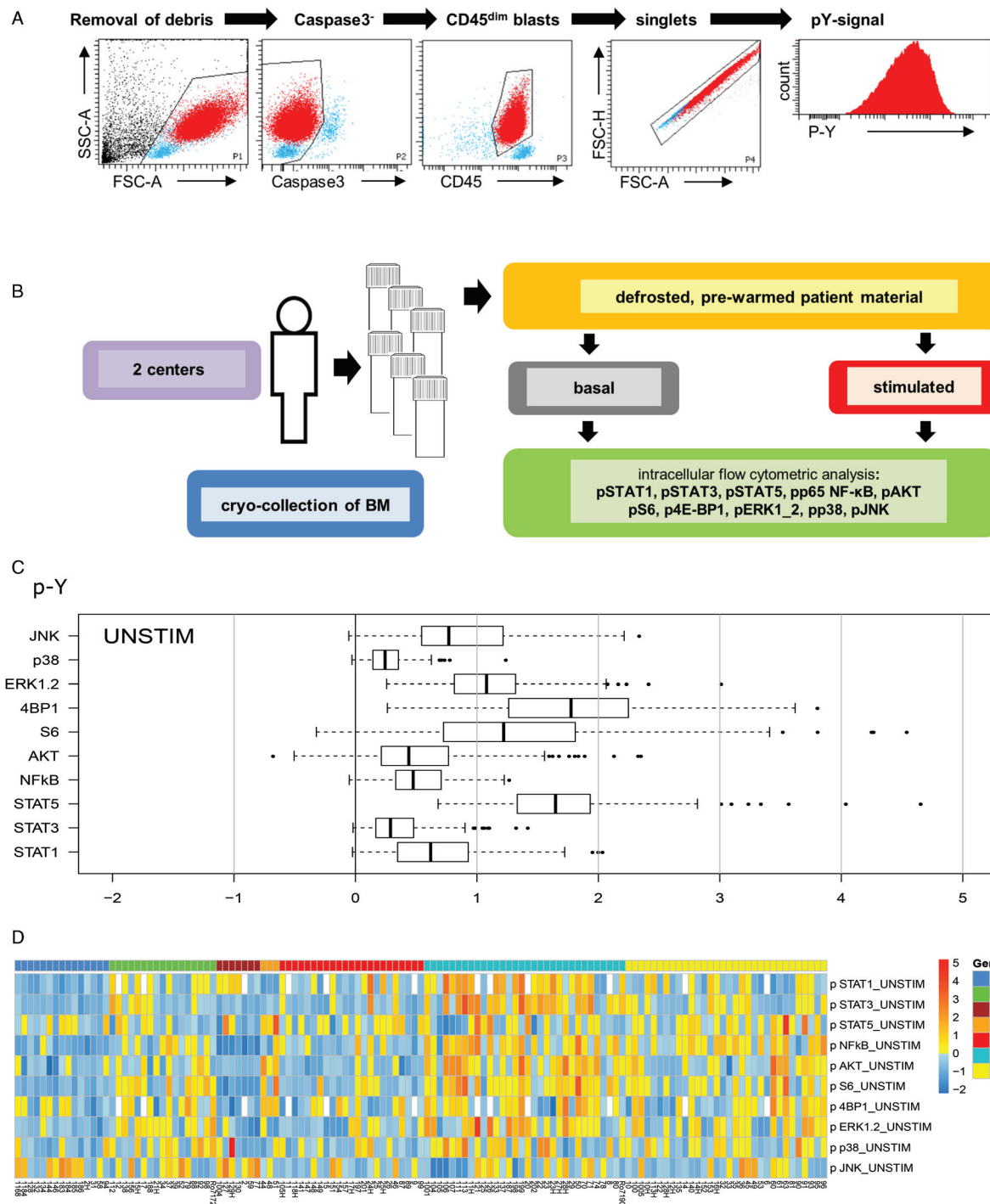
Figure 1. Flow-cytometry screen of phospho-profiles in pedAML under basal conditions. (A) Gating strategy to determine phospho-profiles of pedAML patient samples. (B) Work-flow including sample collection and flow cytometric procedure to determine phospho-profiles of AML patient samples under basal and stimulated condition. (C) The individual basal signal levels of unstimulated AML patient samples (as determined by geoMFI of leukemic cells and represented by raw $\log_2$ of $MFI^{on-target}/MFI^{control}$) are shown. (D) Data of basal phospho-signals per patient plotted according to AML subtypes *RUNX1-RUNX1T1* (n=15); *CBFB-MYH11* (n=17); *PML-RARA* (n=7); *GATA-1* (n=3) gene mutations, patients with normal karyotype (NK; n=23), with *KMT2A* rearrangements (*KMT2Ar*; n=32), and a cohort termed "other" - all other genetic abnormalities (n=32). Individual differences in basal phosphorylation are represented by $\log_2$ ratios of $MFI^{on-target}/MFI^{control}$ which were row-wise scaled in each signal category.

relapsed showed higher signal activation in 11 conditions (independently in the three gross genotypic cohorts: *KMT2A* rearranged (*KMT2Ar*); normal karyotype (NK); with other genetic abnormalities (other), and lower levels in only two signaling nodes (basal pJNK, in all 3 genotypes; basal pSTAT3, only visible in NK and *KMT2Ar*). Phospho-STAT5 was involved in four of the 13 nodes. In univariate analysis with correction for multiple testing (Suppl. Fig. 2D, Supplemental Digital Content,
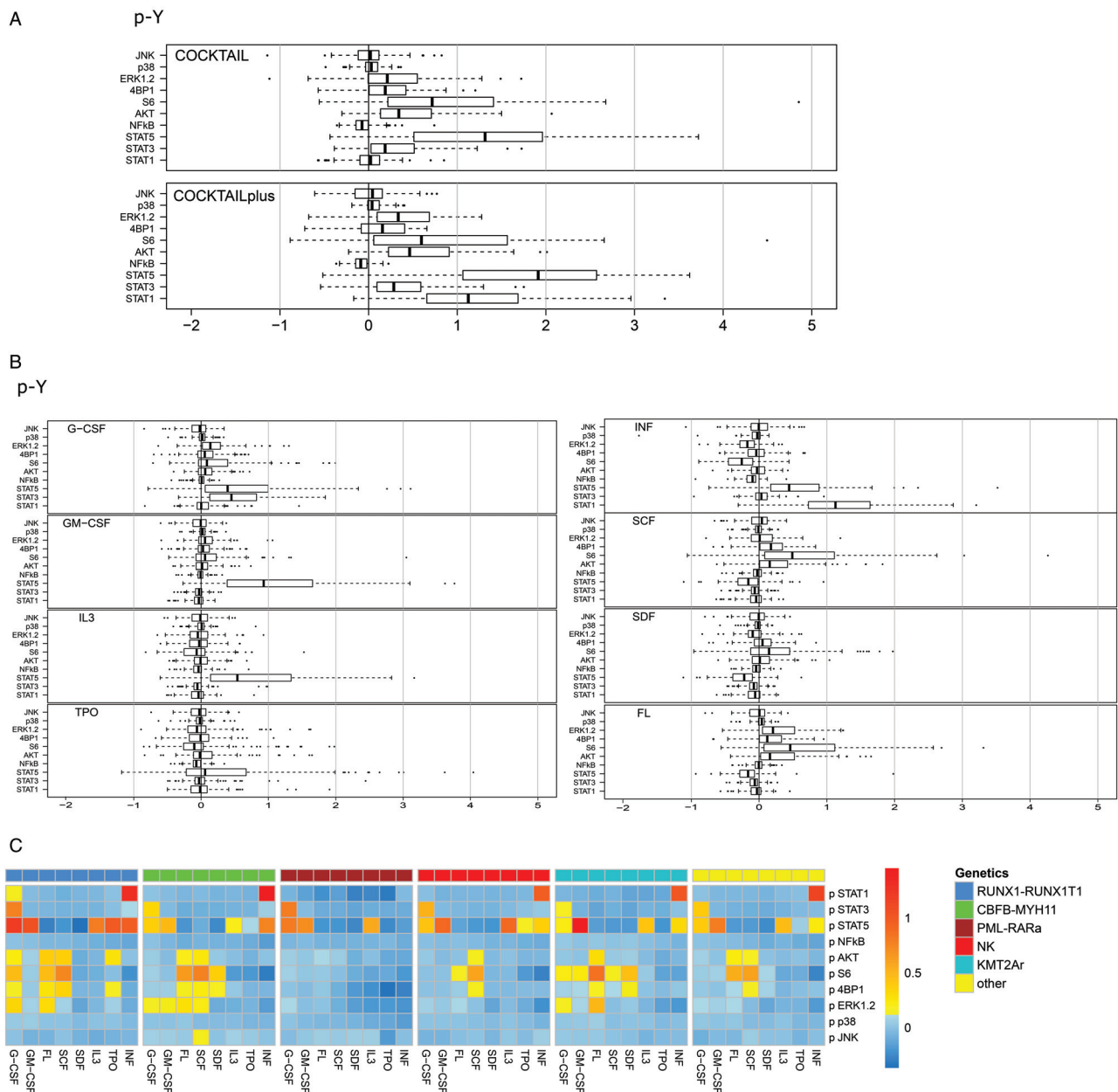
Figure 2. Flow-cytometry screen of phospho-profiles in pedAML under cytokine stimulation. (A) The distribution of signal intensities among leukemic cells of AML patient samples under stimulating culture conditions with "cocktail" or "cocktail plus IFN-γ", or (B) with individual single cytokines are shown. Data are represented by $\log_2$ ratios of the geoMFI$^{on-target}$/geoMFI^{control} of stimulated corrected for unstimulated/basal levels. (C) AML subtype-associated medians of data of each signal node are plotted according to AML subtypes: *RUNX1-RUNX1T1* (n = 15); *CBFB-MYH11* (n = 17); *PML-RARA* (n = 7); patients with normal karyotype (NK; n = 23), *KMT2Ar* (n = 32), and the "other" cohort (n = 32).

http://links.lww.com/HS/A52) as well as in a multivariate model including signal activation nodes and gross genotypic subsets, 2 signal nodes remained of statistical significance (p < 0.01 each; Fig. 3A and Suppl. Fig. 2E, Supplemental Digital Content, http://links.lww.com/HS/A52): GM-CSF/pSTAT5 (HR 3.0; CI 1.5–6.1) and basal pJNK levels (HR 0.3; CI 0.2–0.6).

This prompted us to estimate the cumulative incidences of relapse (CIR; at 5 years) in the total IR/HR cohort of patients according to these two most relevant signal nodes. Patient cohorts were split into 2 groups with low or high signal activation according to thresholds set to median levels of each node. We validated the use of the median as threshold by Cox-regression with restricted cubic splines assessing the potential non-linearity of the relationship between 5-year CIR and signaling node expression level (Suppl. Fig. 3A, Supplemental Digital Content, http://links.lww.com/HS/A52). Basal pJNK^{low} and GM-CSF-stimulated pSTAT5^{high} expressers showed a significantly higher 5-years CIR than reciprocal expressers (p < 0.001 each) (Fig. 3B). This separation of risk groups held true when the three main genetic subgroups were analyzed separately (Suppl. Fig. 3B, Supplemental Digital Content, http://links.lww.com/HS/A52).

Next, we assessed a possible rational association of signal levels with known risk factors including *FLT3*-ITD status as well as white blood cell (WBC) counts at diagnosis tested as
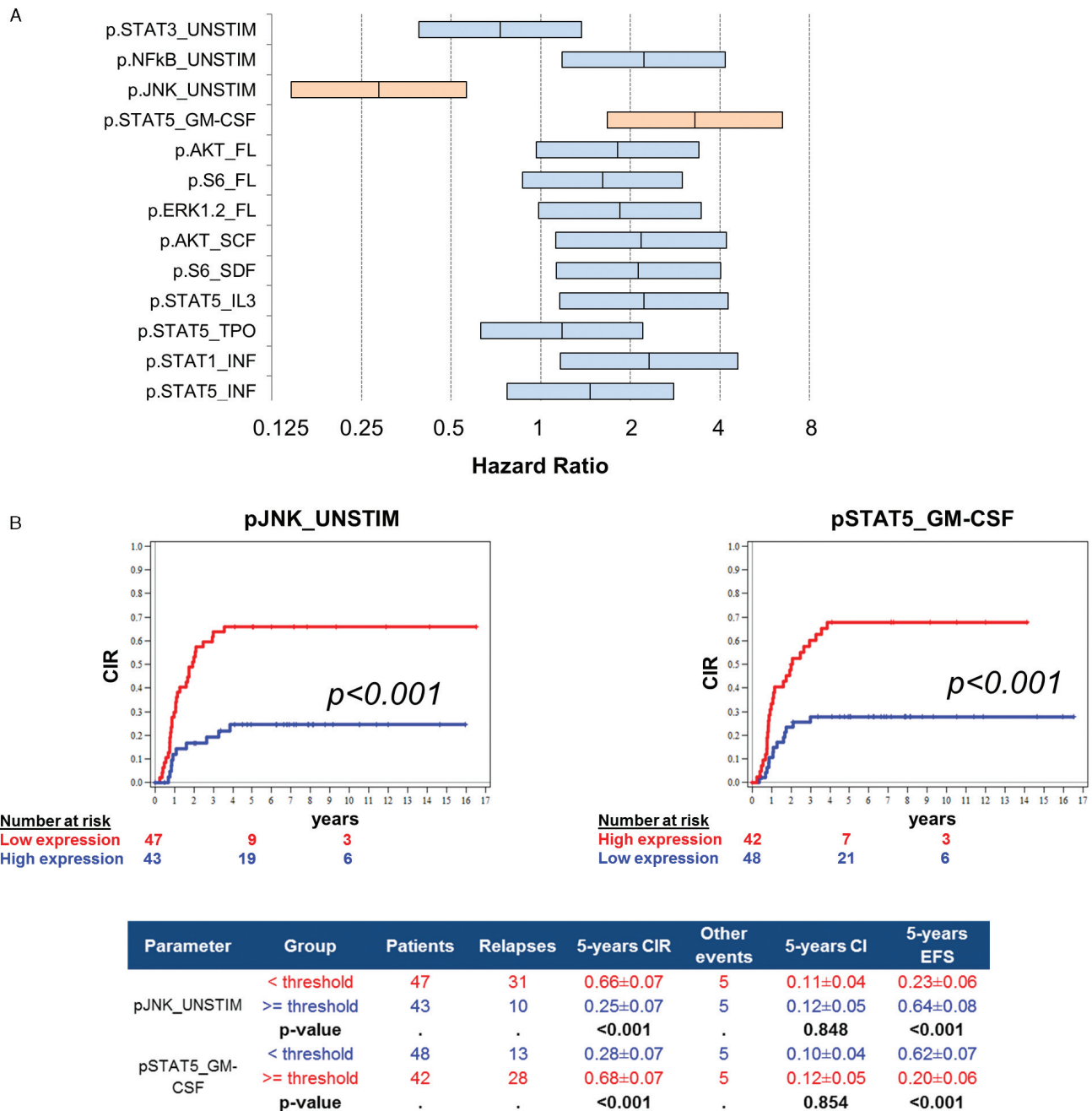
A

B

Parameter	Group	Patients	Relapses	5-years CIR	Other events	5-years CI	5-years EFS
pJNK_UNSTIM	< threshold	47	31	0.66±0.07	5	0.11±0.04	0.23±0.06
	>= threshold	43	10	0.25±0.07	5	0.12±0.05	0.64±0.08
	p-value	.	.	<0.001	.	0.848	<0.001
pSTAT5_GM-CSF	< threshold	48	13	0.28±0.07	5	0.10±0.04	0.62±0.07
	>= threshold	42	28	0.68±0.07	5	0.12±0.05	0.20±0.06
	p-value	.	.	<0.001	.	0.854	<0.001

Figure 3. Levels of pAKT, pSTAT5, pS6 and pJNK predict risk of relapse. (A) Univariate Cox regression analysis was performed to obtain hazard ratios (HR) and 95% confidence interval (CI) for 13 signal nodes with differential phospho-signal activation between samples from relapsed/non-relapsed intermediate and high risk patients. Permutation test was used to adjust for multiple testing. Only the correlations of pJNK_UNSTIM and pSTAT5_GM-CSF with relapse risk remained significant (orange bars), as opposed to the other 11 signal nodes (blue). (B) We merged data from patients of the *KMT2Ar*, NK and "other" groups divided patients into "high" and "low" expressers upon individual magnitude of pSTAT5 (upon GM-CSF) and pJNK (unstimulated) levels. Cut-offs were set using median levels of expressions adjusted according to univariate Cox regression analysis using RCS. 5-years CIR are depicted for pJNK[high] and pJNK[low] as well as for pSTAT5[low] and pSTAT5[high] expressers. (C) Combined assessment of pJNK[low] and pSTAT5[high] in a score-system: 1 point for pJNK[low], 1 additional point for high pSTAT5 levels resulted in three groups with a score of either 0 (none of these factors is present), 1 (either of these factors is present) or 2 (both factors are present). Patients of the "score 2" – group had the highest risk of relapse and the worst 5-years CIR that significantly differed from those of "score 1" or "score 0" cohorts.

continuous variables. As expected, we found that *FLT3*-ITD status (positive in 12/80, 15% of IR/HR patients) significantly correlated in our cohort with the number of relapses, both in the "other" AML subtype (positive in 4/14 relapses; 29%; p < 0.05) as well as in all subtypes together (*KMT2Ar*+NK+other; positive 9/41 relapses; 22%; p < 0.05). However, there was no correlation of the *FLT3*-ITD status with basal pJNK or GM-CSF/

pSTAT5 levels (Suppl. Fig. 4A and B, Supplemental Digital Content, http://links.lww.com/HS/A52). Data on *NPM1* mutations were not available. Higher WBC counts, another known risk factor, did not correlate with adverse signal activation of the driver signal represented by high GM-CSF/pSTAT5 levels (Suppl. Fig. 4C, Supplemental Digital Content, http://links.lww.com/HS/A52).
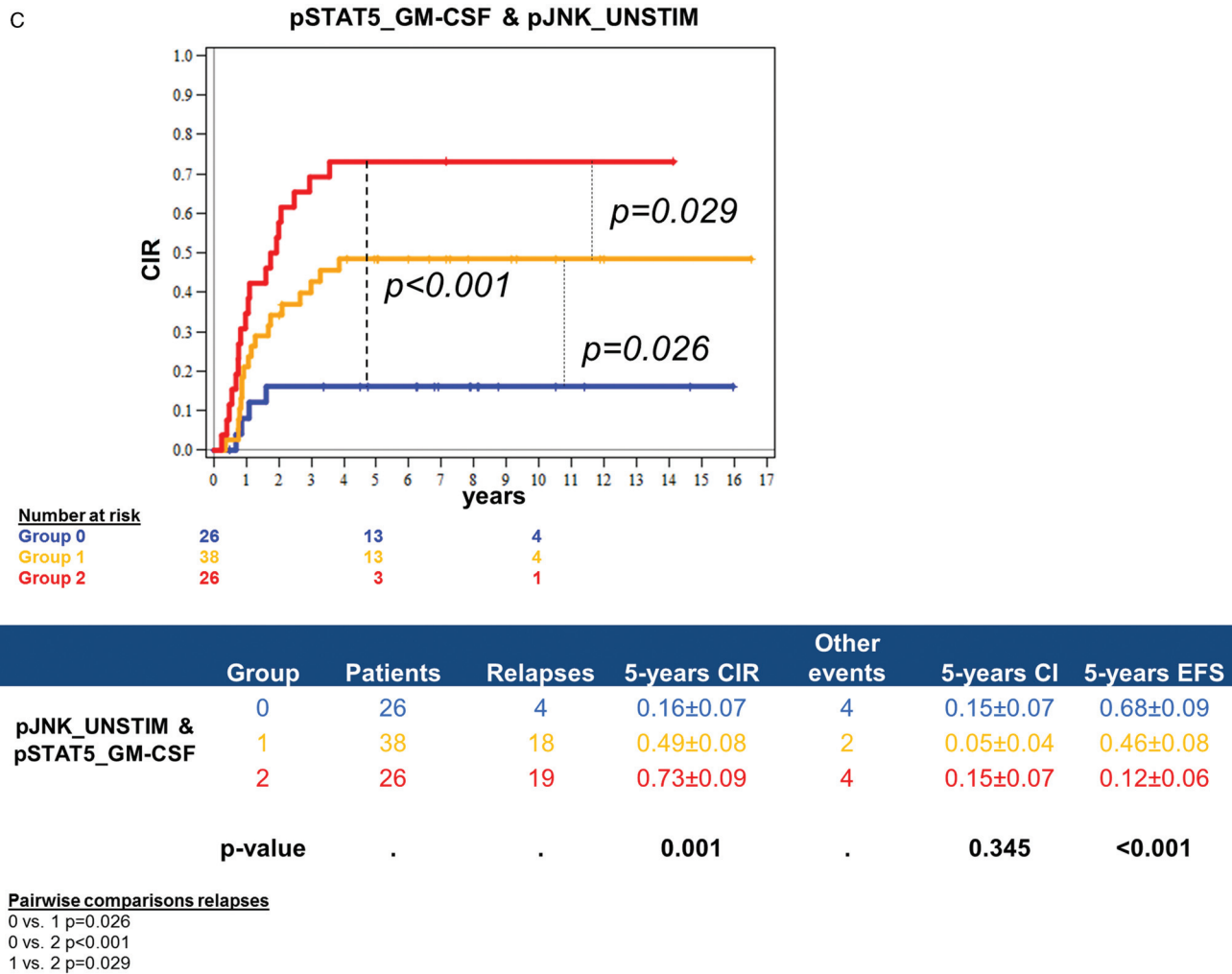
C

pSTAT5_GM-CSF & pJNK_UNSTIM

Number at risk

Group 0	26	13	4
Group 1	38	13	4
Group 2	26	3	1

	Group	Patients	Relapses	5-years CIR	Other events	5-years CI	5-years EFS
pJNK_UNSTIM & pSTAT5_GM-CSF	0	26	4	0.16±0.07	4	0.15±0.07	0.68±0.09
	1	38	18	0.49±0.08	2	0.05±0.04	0.46±0.08
	2	26	19	0.73±0.09	4	0.15±0.07	0.12±0.06
	p-value	.	.	0.001	.	0.345	<0.001

Pairwise comparisons relapses
0 vs. 1 p=0.026
0 vs. 2 p<0.001
1 vs. 2 p=0.029

Figure 3. (Continued).

To analyze whether the combined assessment of the two most relevant signaling nodes is of additive prognostic value we established a score-system according to the result of the Cox-regression: 1 point each for pJNK^{low} or GM-CSF/pSTAT5^{high} levels. This resulted in 3 groups with significantly different relapse rates (5y CIR score 0: 0.16 ± 0.07; score 1: 0.49 ± 0.08; score 2: 0.73 ± 0.09) (Fig. 3C).

Phospho-flow and functional testing of inhibitor sensitivity

We further applied phospho-flow to primary AML blasts treated with a set of FDA approved signal inhibitors to test whether individual drug-sensitivity can be predicted by measuring phospho-levels at the time of diagnosis, and/or by changes of phospho-levels upon in vitro drug treatment. We focused on ruxolitinib, dasatinib, midostaurin, sorafenib, sunitinib, rapamycin, everolimus, bortezomib, and erlotinib which all are either used or suggested for treatment of AML. Later in the study we expanded the inhibitor panel and added the in vitro-only inhibitor AG490 along with ruxolitinib because their specificity for JAK-signaling is potentially relevant for AML. Inhibitor sensitivity in terms of in vitro reduction of viable AML blasts (Suppl. Fig. 5A, Supplemental Digital Content, http://links.lww.

com/HS/A52) was assessed along with signal expressions in 44 primary AML samples (Suppl. Fig. 5B, Supplemental Digital Content, http://links.lww.com/HS/A52) out of the total cohort.

Midostaurin was most effective in reducing viable AML blasts (Fig. 4A and Suppl. Fig. 5C, Supplemental Digital Content, http://links.lww.com/HS/A52) in 25 of 44 cases irrespective of the AML subtype (genetic or FAB type, Fig. 4B). Similar effects were only seen upon AG490 treatment which also evoked responses (in 8/29 tested samples) throughout all FAB subtypes (mainly in *KMT2Ar* and NK subgroups).

Midostaurin was also most active in reducing several signals like pS6, pSTAT5 and pAKT (Fig. 4C). However, phospho-signal levels at diagnosis did not indicate inhibitor sensitivity (Suppl. Figs. 6A and 6B, Supplemental Digital Content, http://links.lww.com/HS/A52), and the extent of modulation of phospho-levels by inhibitors did not necessarily predict the degree of reduction of viable AML blasts (Fig. 4C and Suppl. Figs. 7 and 8, Supplemental Digital Content, http://links.lww.com/HS/A52).

Xenotransplant validation of signaling inhibitor sensitivities

To validate the efficacy of signaling inhibitor treatment in vivo, we performed xenotransplantation experiments in mice (scheme
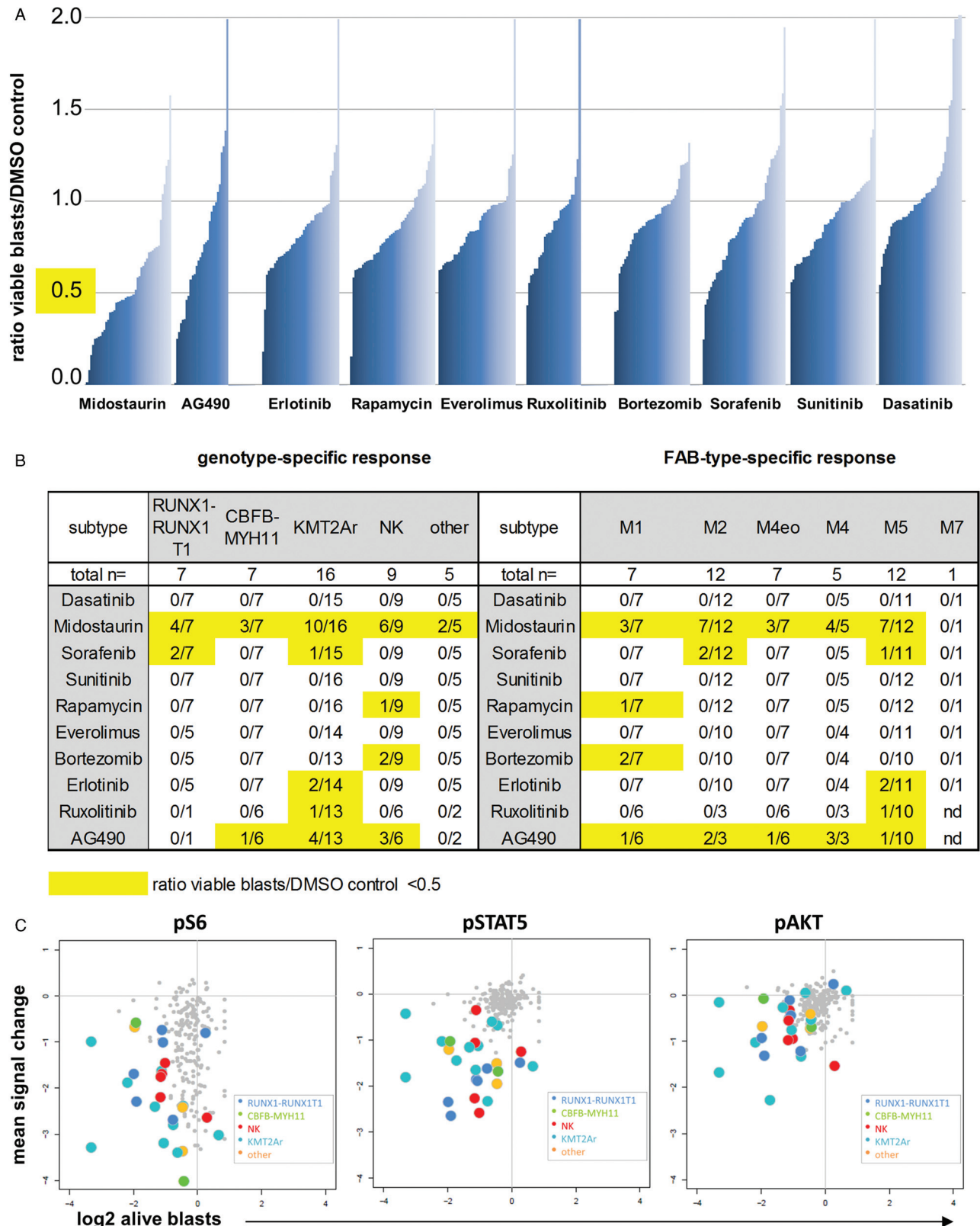
Figure 4. Midostaurin treatment kills pedAML blasts and lowers pS6, pSTAT5 and pAKT levels. (A) Histogram showing the sensitivity of AML blasts towards individual signaling inhibitors (ruxolitinib n=28, AG490 n=28, dasatinib n=43, midostaurin n=44, erlotinib n=40, rapamycin n=44, everolimus n=40, bortezomib n=39, sorafenib n=43, sunitinib n=44). Number of alive blasts following signaling inhibitor treatment was assessed using YO-PRO™ apoptotic cell staining and subsequent flow cytometric analysis. Ratio of alive blasts following signaling inhibitor treatment versus vehicle (DMSO) control is shown. (B) Responses of AML blasts to signaling inhibitors according to genetic categories and FAB subtypes. A ratio <0.5 (viable blasts^inhibitor/viable blasts^DMSO) was considered as response. (C) The magnitude of reduction of pS6, pSTAT5 and pAKT (y-axis) following treatment with midostaurin (color) or other signaling inhibitors (grey) and the association with the number of alive blasts (x-axis) is depicted for the different genetic AML subtypes (depicted in different colors).
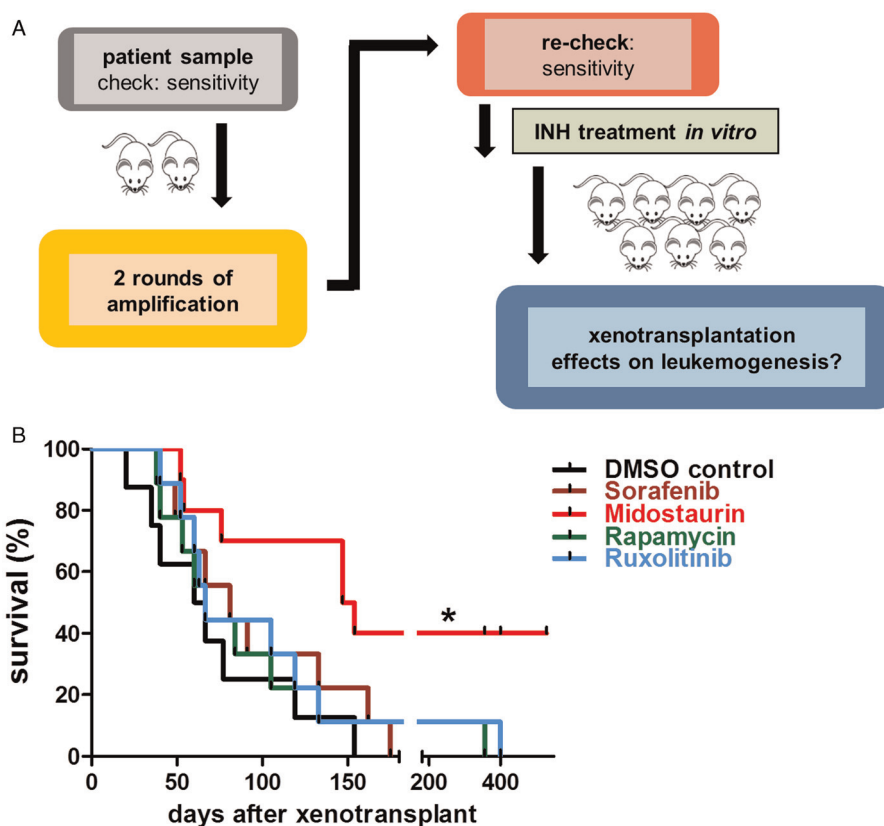
Figure 5. **Midostaurin treatment prolongs survival of xenotransplanted mice**. (A) Scheme of the experimental setup. (B) Samples from each AML patient were injected into NSG mice for cell amplification, then divided into 5 experimental groups to be treated ex-vivo either with sorafenib, midostaurin, rapamycin, ruxolitinib or DMSO and again injected into NSG mice. Survival of the xenografted mice according to experimental groups (sorafenib, rapamycin, ruxolitinib, midostaurin, and DMSO control). p values from a Log-rank (Mantel-Cox) Test.

Fig. 5A). Expanded blasts from 5 *KMT2Ar* patients (Suppl. Fig. 9A, Supplemental Digital Content, http://links.lww.com/HS/A52) were divided into 5 experimental groups (sorafenib, midostaurin, rapamycin, ruxolitinib and DMSO [vehicle] control), pretreated (overnight) ex vivo and injected into NSG mice. Major shifts of drug sensitivities due to cell expansion in mice were excluded before (Suppl. Fig. 9B, Supplemental Digital Content, http://links.lww.com/HS/A52). The presence of human CD45^{+} (hCD45^{+}) cells in the peripheral blood of mice was monitored over time (Suppl. Fig. 9C, Supplemental Digital Content, http://links.lww.com/HS/A52). Complete time courses were obtained from three individual patients. In all settings, treatment of midostaurin significantly delayed the expansion of hCD45^{+} cells. Assessment of hCD45+ cells in the bone marrow (Suppl. Fig. 9D, Supplemental Digital Content, http://links.lww. com/HS/A52) and spleen (data not shown) at the time of terminal disease showed a pronounced high grade leukemic cell infiltration. Whereas survival of the xenografted mice upon sorafenib-, rapamycin- and ruxolitinib-treatment was unaltered compared to the DMSO control, midostaurin treatment significantly prolonged disease latency (Fig. 5B).

Discussion

Our study demonstrates that phospho-flow of primary AML blasts can complement and expand on known prognostic information of pedAML, and is potentially useful to refine current risk assessment strategies and tailor individual therapy.

We investigated the activation status of representative key molecules (STAT3, STAT5, ERK1/2, JNK, p38, and AKT) of the three major signaling pathways related to leukemogenesis, that is, the JAK/STAT, RAF/MEK/ERK (MAPK) and the PI3K/AKT/mTOR pathway.[21–27] Most signals delivered by cytokines, or by mutant receptors (eg, FLT3, c-KIT) converge to these molecules, and many new inhibitory agents (like sunitinib, sorafenib, dasatinib) act up-stream of them. NFκB and S6 ribosomal protein act further downstream and confer anti-apoptotic as well as growth-regulating effects. They are activated in AML by the ERK- and in particular by the PI3K/AKT pathway, and may serve as secondary read-out markers of these pathways. Hence, we considered these molecules to be ideal points of convergence for activated signal pathway profiling. All phosphorylation sites examined in the study are indicative for the activation of the given molecules (Suppl. Table 2, Supplemental Digital Content, http://links.lww.com/HS/A52). Several other studies already reported aberrant constitutive activation of individual signaling molecules in AML.[28–34] Our study now gives a comprehensive overview on key signaling pathways in pedAMLs with respect to genotype-related heterogeneities. Basal activation of pSTAT5 was found throughout all pedAML subtypes, whereas the basal activation of other signaling molecules differed according to genotypes. The *KMT2Ar* group was characterized by broadest basal signal activation – similarly as described in,[35] followed by the "other" and *CBFB-MYH11* groups. In contrast, *RUNX1-RUNX1T1* and *PML-RARA* subsets were comparably silent except for pJNK activation. Elevated pSTAT5 signaling elicited by several

cytokines was found to be a general hallmark of pedAML with strongest stimulation through GM-CSF, which mirrors observations in chronic myeloid malignancies.[36,37] STAT3 activation by G-CSF was also a consistent finding throughout all subtypes as described before,[11] whereas cytokine-stimulated patterns of pAKT, pS6, p4E-BP1, pERK1/2 rendered genotype associated signatures.

Both, constitutive or triggered activation of certain signaling molecules like pAKT, pERK, and pSTAT5 has been assigned prognostic relevance in adult myeloid malignancies.[33,38] In pedAML, G-CSF/IL6 sensitivity of STAT3 signaling and elevated STAT3 sensitivity were found to correlate with good prognosis and low risk genotypes.[11] Our data confirm previous observations including the fact that broadly elevated signal activation except for pSTAT3 correlates with relapses. High levels of GM-CSF-stimulated pSTAT5 and low basal levels of pJNK were the most significant parameters correlating with increased relapse incidence. This was particularly true for patients with higher clinical risk (subgroups *KMT2Ar*, NK and "other"). To date most studies have focused on molecular and genetic lesions[39–41] for stratifying patients with AML, but outcome as well as relapse risk vary considerably within IR and HR groups.[42,43] We propose that the combination of these two outcome-predicting signal activation nodes allows separating three distinct risk groups among IR and HR pedAMLs. Testing these parameters at initial diagnosis fuels the possibility of improving stratification by applying phospho-flow. Our data also corroborate that interfering with pSTAT5 may be a broadly applicable signal-dependent intervention strategy against pedAML regarding its salient activation patterns.

To explore further potential applications of phospho-flow we assessed whether the activation status of signaling molecules at diagnosis or their modulation upon treatment with different FDA approved signaling inhibitors predicts drug-responsiveness of AML blasts. We found that neither was the activation of a specific signaling molecule predictive for the cytotoxic efficacy of any of the inhibitors used in our ex vivo short-term drug sensitivity assay, nor was the cytotoxic efficacy of a certain drug exactly predicted by phospho-signal inhibition of singly investigated signaling molecules. We could, however, demonstrate that midostaurin displayed the broadest and most consistent cytotoxic effects as compared to the other inhibitors tested against various genetic subtypes of pedAML including a larger cohort of *KMT2Ar* cases. Interestingly, midostaurin in particular showed also simultaneous suppressive activity against several signaling molecules implicated above in prognostic aspects (pSTAT5, pAKT, pS6). Other drugs appeared to exert less or more selective activity.

The relevance of our ex vivo drug sensitivity assay was further validated in a murine xenograft model of *KMT2Ar* pedAML. Herein, again midostaurin showed efficacy in suppressing leukemic engraftment, thus exerting some activity probably even on the leukemic stem-cell level in *KMT2Ar* AML. Although further investigations are necessary to draw definite conclusions, one could speculate that the superior activity of midostaurin could be a result of multi-kinase signaling interception. Most cancer cells are not addicted to a single overactive kinase pathway and the vast majority of so called "specific kinase inhibitors" exert considerable off-target effects. This is also consistent with the emerging view that sensitivity to an inhibitor may not only be due to activation of the target kinase but also to activation of multiple parallel pathways.[44] Accordingly, we demonstrate that a functional phenotype-driven ex vivo drug testing approach such

as the one presented here is more likely to lead to identification of effective drugs than a purely hypothesis-driven, genomic target-centric approach.[45,46]

Our investigation has some limitations, including its basic design as a single-laboratory, retrospective study on frozen samples of patients recruited over two full clinical trial periods, during which some changes of diagnostic approaches, stratification and treatment have been made. A full characterization of genetic and molecular features, as would be nowadays necessary for separating three risk groups[14,15] was not available. Hence, we summarized IR and HR patients together. Notwithstanding this, we find it striking that a single test still can separate patients at risk well in this otherwise mixed cohort of cases. A more detailed investigation of the capabilities of the test within well-defined genetic subgroups needs to be performed anyway on a much larger, independent cohort and in a multi-centric fashion to warrant implementation into future up-front stratification schemes of pedAML for further treatment personalization. To this end, preliminary technical data confirm that flow-cytometric assessment of phospho-levels on thawed material (as in this study) or on fresh samples renders largely concordant results (Suppl. Fig. 10, Supplemental Digital Content, http://links.lww.com/HS/A52). Obviously, also our cytotoxicity-oriented drug sensitivity assay has limitations related to usage of single drug concentrations which were, however, oriented on human pharmacokinetic data, as well as to its short-term design probably unable to detect effects not linked with immediate cytotoxic effects. The amazing similarity with the results of xenograft models, still appear to indicate some biologic substance.

We conclude that phospho-flow and the functional phenotype-driven drug sensitivity assay yielded critical insights into potential novel options for improved relapse-risk assessment, stratification, as well for guiding personalized therapy, and should therefore be further validated in pedAML.

Materials and methods

Patients and cells

Sampling as well as subsequent research was covered by appropriate informed consent policies and clearance of study procedures by the involved ethical committees. We analyzed BM samples (cryopreserved after gradient-centrifugation) from 166 newly diagnosed pedAML patients recruited to the AML-BFM-1998 and 2004 treatment protocols in Austria (n = 132; assessed as per availability of frozen samples out of the total cohort of 191 registered patients in the trial periods) and Germany (n = 34; randomly selected upon sample availability). The median age of patients was 10.06 years (range 0.17–17.88), and the initial leukocyte count was 35 G/L in median (range 0.93–521.1 G/L). BM sampling was done as clinically indicated per protocol. We used only leftover materials stripped from further clinical questions. Sampling as well as subsequent research was covered by appropriate informed consent policies and clearance of study procedures by the involved ethical committees. Clinical data including detailed genetic information, events and outcome in long-term follow-up were also collected and were complete in 132 patients (79.5%). Among those 132 patients there were 42 patients fulfilling LR (low/standard risk) criteria as per protocol [*RUNX1-RUNX1T1* (n = 15); *CBFB-MYH11* (n = 17); *PML-RARA* (n = 7); *GATA-1* (n = 3, all are children with Down syndrome) gene mutations], as well as 90 patients with

intermediate or high risk (IR/HR) criteria[1,2] [*KMT2A* rearrangements (n = 33); normal karyotype (NK; n = 23); as well as a remaining cohort with variable genetics - termed "other" (n = 34)]. Treatment details of trials AML-BFM-1998 and 2004 have been delineated previously.[1,2] The entire cohort of non-LR patients was summarized as IR/HR patient cohort in order to represent what would nowadays be stratified separately. All cases of the *KMT2Ar* group (Suppl. Fig. 2B, Supplemental Digital Content, http://links.lww.com/HS/A52) were treated in the HR group of the respective protocols. Only later after stop of recruitment to the presented study, such patients were split into an IR and HR group, respectively, dependent on the type of *KMT2A*-rearrangement which is current BFM strategy. *FLT3*-ITD data were available in a subset of 97 patients; no other mutational results were available due to the retrospective nature of the study. There was no significant difference between the analysed cohort and all registered patients in Austria regarding risk group allocation (LR: 31.8% vs 38.1%; n.s.; IR/HR: 68.2% vs 61.9%; n.s.) as well as regarding relapse rates (34.1% vs. 33.7%). The median follow-up time in analyzed patients without a relapse was 6.25 years (range 0.0–16.5 years). See Suppl. Table 1 (Supplemental Digital Content, http://links.lww.com/HS/A52) for details on patient characteristics.

Phospho-Flow for measurement of basal and cytokine stimulated signaling

Cryopreserved AML samples were thawed, split in 1×10^6 cells/ml aliquots, incubated for 2 hours in serum-free X-Vivo[TM] 10 medium (Lonza) and stimulated with 20 ng/ml of either G-CSF, GM-CSF, FL, SCF, SDF1, IL-3, TPO, or IFN-γ, or with a mixture of cytokines (all from Peprotech) without ("cocktail") and with IFN-γ ("cocktail plus") at a common cytokine concentration of 1 ng/ml (except G-CSF: 5 ng/ml) for 15 minutes at 37°C, or left untreated, respectively. Cells were then fixed with 2% formaldehyde (free of MeOH; Polyscience or Thermoscientific) for 15 min at RT and permeabilized in 100% ice-cold MeOH for 15 minutes at −20°C. Cells were centrifuged, MeOH was completely removed and the pellet was washed once and resuspended in PBS/1% human serum albumin. The cell suspension was split into seven micronic tubes and labelled for flow cytometry with CD45, anti- active caspase-3 and with antibodies against respective phospho-sites (see Suppl. Table 2, Supplemental Digital Content, http://links.lww.com/HS/A52, for details on antibodies). All phosphorylation sites examined in the study are indicative for the activation of the given molecules (see Suppl. Table 2, Supplemental Digital Content, http://links.lww.com/HS/A52, for respective references). Cells were stained for 30 min at RT and analyzed by flow cytometry (FACSCalibur, BD). Only viable (according to scatter properties and negativity by anti- active caspase 3 staining) leukemic blasts (median 71%; range 30%–91%) were analyzed by gating on low/intermediate-side scatter cells with low CD45 expression, thus excluding active caspase 3-positive blasts (median 7%; range 1%–35%) as well as residual normal cells.

Phospho-Flow for measurement of signaling inhibition and flow-cytometric cell survival assay

Approximately 1×10^6 cells/ml were incubated for 2 hours with one of the respective signaling inhibitors (see Suppl. Table 3, Supplemental Digital Content, http://links.lww.com/HS/A52) in serum-free X-Vivo[TM] 10 medium at 37°C followed by 15 minutes

stimulation with added cytokine cocktail (as above). DMSO (vehicle) treatment together with cytokine cocktail was used as control. Fixation, permeabilization, staining of the cells and flow-cytometric measurement of phospho-levels were performed as described above. In parallel to flow cytometric measurement of phospho-levels after 2 hours signaling inhibitor treatment, we performed an in vitro cell survival assay. For this purpose, sample aliquots containing 1×10^6 cells were incubated for 48 hours with individual signaling inhibitors (selection and concentrations as described above) in serum-free X-Vivo[TM] 10 medium supplemented with cocktail and kept at 37°C in a humidified atmosphere of 5% CO_2. Cells treated with DMSO instead of inhibitor were used as controls. After 48 hours, cells were incubated for 1 hour by adding 1 μg/ml of Vybrant violet stain (freely cell-permeable DNA-dye for cell cycle profiling; Invitrogen/#V35003) to otherwise untouched incubations. Subsequently, entire cell incubations were transferred into BD Trucount Tubes[TM] (for bead-based absolute counting) and YO-PRO[TM]-1 Iodide (10 μg/ml; apoptotic cell dye; ThermoFisher Scientific) as well as CD45 PerCP-CY5.5 antibody (as before) were added. Measurement and analysis were performed subsequently without a centrifugation step on a BD LSR2 Flow Cytometer equipped with a violet laser using BD FACSDiva software. Absolute viable blast counts (CD45^{low}SSC^{low}YO-PRO1[negative]) were calculated upon individual tube-specific bead-based correction factors.

Xenotransplantation and in vivo drug studies

NOD.*SCID*-IL2Rγ[null] (NSG) mice were bred and maintained under specific pathogen-free conditions according to FELASA recommendations. Breeding and experiments were approved by the Ethics and Animal Welfare Committee of the University of Veterinary Medicine Vienna and granted by the national authority (Austrian Federal Ministry of Science and Research) according to Section 8ff of Law for Animal Experiments under licenses BMWFW-68.205/0112-WF/V/3b/2016 and BMWFW-68.205/0093-WF/V/3b/2015 and were performed according to the guidelines of FELASA and ARRIVE. Schematic presentation of the experiment is presented in Figure 5A. Patient-derived AML samples were thawed, washed once with PBS, split into three and injected intravenously into NSG mice for cell amplification. Human cell engraftment was evaluated by the presence of human CD45 positive cells in mouse blood using anti-mouse CD45-PE-Cyanine7 (30-F11; ThermoFisher Scientific, eBioscience[TM] #25-0451-81) versus anti-human CD45-eFluor 450 (HI30; ThermoFisher Scientific, eBioscience[TM] #48-0459-42). Flow-cytometric measurement was performed on a BD FACSCanto II (BD Bioscience, Heidelberg, Germany) and data analyzed using BD FACSDiva software V8.0. After successful engraftment mice were sacrificed by cervical dislocation. Single cell suspensions were obtained by pressing the spleen trough 100 μm cell strainers or flushing the BM. Cell suspensions of mice containing engrafted patient leukemic cells were frozen in freezing medium containing 10% DMSO and 90% FCS (Capricorn, #FBS-12A) until further usage or injected for further amplification into NSG mice.

For validation of signaling inhibitor sensitivity of AML blasts in vivo murine splenic cell suspension containing engrafted human leukemic cells were split into five experimental groups and incubated with selected signaling inhibitors (midostaurin, rapamycin, ruxolitinib, sorafenib; at concentrations as described in Material and Methods) or DMSO (vehicle) as negative control in X-Vivo[TM] 10 overnight at 37°C prior to intravenous injection into NSG mice (approximately 2×10^5 cells/mouse; 2 mice/

inhibitor; 2 independent experiments). Disease onset was monitored by puncturing vena facialis and blood analysis of human CD45 cells as described above. Leukemic mice were sacrificed by cervical dislocation. Patient leukocytes in blood and singe cell suspensions of spleen and bone marrow were analyzed as described above.

Statistical analysis

Basal and induced signal protein phosphorylation was assessed according to a method adapted from Irish and Nolan et al.[47] using log_2 ratios of geometric mean fluorescence intensities (geoMFI) of target expressions versus mock control. Signal assays were performed blinded regarding clinical outcome data. Differences in the distribution of features between groups of patients were investigated using the Chi-Square test (contingency tables with continuity correction).

The construction of a heatmap was performed in R statistical environment using the "pheatmap" package. For hierarchical clustering "euclidean distance" and the "complete clustering" algorithm was used.

For the evaluation of the prognostic value of the signals, signals were dichotomized using the median as threshold. To screen for relevant differences of signal activation in correlation with relapses we performed univariate analysis in the framework of a Cox regression with the competing events (non-leukemic death, stem cell transplantation without subsequent relapse) censored. Adjusted p-values were derived using the Permutation test to correct for multiple testing. Multivariate analysis was restricted to eleven signal nodes as, as pSTAT1_IFN and pSTAT5_IFN were missing in 12/90 patients. Restricting the analysis to eleven nodes allowed evaluation of 88 patients. We used the multivariable Cox-model for cause-specific hazard ratios with backward stepwise selection with a p-value greater than 0.05 for removal of variables, where genetic subtype was forced into the model. Bootstrapping was used to estimate the amount of required shrinkage to account for overfitting.[48]

Cumulative incidence of relapses (CIR) was estimated taking into account the competing events calculated from the respective time-point of assessment until the date of event or last observation. The CIR was compared with the Gray test.[49] All CIR estimates were set to 5 years of observation. Secondary endpoint was event-free survival (EFS) estimated according the method of Kaplan-Meier. In order to validate using the median as threshold, Cox-regression with restricted cubic splines was used to univariately estimate a potential non-linear relationship between the signal level and the cause-specific hazard ratios and the estimated 5-year CIR.[50]

Acknowledgments

References

1. Boztug H, Mühlegger N, Glogova E, et al. Development of treatment and clinical results in childhood AML in Austria (1993–2013). *Memo.* 2014;7:63–74.
2. Rasche M, Zimmermann M, Borschel L, et al. Successes and challenges in the treatment of pediatric acute myeloid leukemia: a retrospective analysis of the AML-BFM trials from 1987 to 2012. *Leukemia.* 2018;32:2167–2177.
3. Kornblau SM, Womble M, Qiu YH, et al. Simultaneous activation of multiple signal transduction pathways confers poor prognosis in acute myelogenous leukemia. *Blood.* 2006;108 7:2358–2365.
4. Stone RM, Mandrekar SJ, Sanford BL, et al. Midostaurin plus Chemotherapy for Acute Myeloid Leukemia with a FLT3 Mutation. *N Engl J Med.* 2017;377 5:454–464.
5. Rollig C, Serve H, Huttmann A, et al. Addition of sorafenib versus placebo to standard therapy in patients aged 60 years or younger with newly diagnosed acute myeloid leukaemia (SORAML): a multicentre, phase 2, randomised controlled trial. *Lancet Oncol.* 2015;16 16:1691–1699.
6. Sallman DA, Lancet JE. What are the most promising new agents in acute myeloid leukemia? *Curr Opin Hematol.* 2017;24 2:99–107.
7. Larrosa-Garcia M, Baer MR. FLT3 inhibitors in acute myeloid leukemia: current status and future directions. *Mol Cancer Ther.* 2017;16 6:991–1001.
8. Fischer T, Stone RM, Deangelo DJ, et al. Phase IIB trial of oral Midostaurin (PKC412), the FMS-like tyrosine kinase 3 receptor (FLT3) and multi-targeted kinase inhibitor, in patients with acute myeloid leukemia and high-risk myelodysplastic syndrome with either wild-type or mutated FLT3. *J Clin Oncol.* 2010;28:4339–4345.
9. Cortes JE, Perl AE, Dombret H, et al. Final results of a phase 2 open-label, monotherapy efficacy and safety study of quizartinib (AC220) in Patients ≥ 60 years of age with FLT3 ITD positive or negative relapsed/refractory acute myeloid leukemia. *Blood.* 2012-;120:48–148.
10. Letai A. Functional precision cancer medicine-moving beyond pure genomics. *Nature Med.* 2017;23 9:1028–1035.
11. Redell MS, Ruiz MJ, Gerbing RB, et al. FACS analysis of Stat3/5 signaling reveals sensitivity to G-CSF and IL-6 as a significant prognostic factor in pediatric AML: a Children's Oncology Group report. *Blood.* 2013;121:1083–1093.
12. Chen WC, Yuan JS, Xing Y, et al. An integrated analysis of heterogeneous drug responses in acute myeloid leukemia that enables the discovery of predictive biomarkers. *Cancer Res.* 2016;76:1214–1224.
13. Schaab C, Oppermann FS, Klammer M, et al. Global phosphoproteome analysis of human bone marrow reveals predictive phosphorylation markers for the treatment of acute myeloid leukemia with quizartinib. *Leukemia.* 2014;28:716–719.
14. Zwaan CM, Kolb EA, Reinhardt D, et al. Collaborative Efforts Driving Progress in Pediatric Acute Myeloid Leukemia. *J Clin Oncol.* 2015;33:2949–2962.
15. Creutzig U, van den Heuvel-Eibrink MM, Gibson B, et al. Diagnosis and management of acute myeloid leukemia in children and adolescents: recommendations from an international expert panel. *Blood.* 2012;120:3187–3205.
16. Kaushansky K. Lineage-specific hematopoietic growth factors. *N Engl J Med.* 2006;354:2034–2045.
17. Wodnar-Filipowicz A, Lyman SD, Gratwohl A, et al. Flt3 ligand level reflects hematopoietic progenitor cell function in aplastic anemia and chemotherapy-induced bone marrow aplasia. *Blood.* 1996;88:4493–4499.
18. Bruserud O, Foss B, Petersen H. Hematopoietic growth factors in patients receiving intensive chemotherapy for malignant disorders: studies of granulocyte-colony stimulating factor (G-CSF), granulocyte-macrophage colony stimulating factor (GM-CSF), interleukin-3 (IL-3) and Flt-3 ligand (Flt3L). *Eur Cytokine Netw.* 2001;12:231–238.
19. Lyman SD, Jacobsen SE. c-kit ligand and Flt3 ligand: stem/progenitor cell factors with overlapping yet distinct activities. *Blood.* 1998;91:1101–1134.
20. Reisbach G, Kamp T, Welzl G, et al. Regulated plasma levels of colony-stimulating factors, interleukin-6 and interleukin-10 in patients with acute leukaemia and non-hodgkin's lymphoma undergoing cytoreductive chemotherapy. *Br J Haematol.* 1996;92:907–912.
21. Platanias LC. Map kinase signaling pathways and hematologic malignancies. *Blood.* 2003;101:4667–4679.
22. Chang F, Steelman LS, Lee JT, et al. Signal transduction mediated by the Ras/Raf/MEK/ERK pathway from cytokine receptors to transcription factors: potential targeting for therapeutic intervention. *Leukemia.* 2003;17:1263–1293.

23. Chang F, Lee JT, Navolanic PM, et al. Involvement of PI3K/Akt pathway in cell cycle progression, apoptosis, and neoplastic transformation: a target for cancer chemotherapy. *Leukemia.* 2003;17:590–603.

24. Rane SG, Reddy EP. JAKs, STATs and Src kinases in hematopoiesis. *Oncogene.* 2002;21:3334–3358.

25. Dinner S, Platanias LC. Targeting the mTOR Pathway in Leukemia. *J Cell Biochem.* 2016;117:1745–1752.

26. Jain N, Curran E, Iyengar NM, et al. Phase II study of the oral MEK inhibitor selumetinib in advanced acute myelogenous leukemia: a University of Chicago phase II consortium trial. *Clin Cancer Res.* 2014;20:490–498.

27. Lunghi P, Tabilio A, Dall'Aglio PP, et al. Downmodulation of ERK activity inhibits the proliferation and induces the apoptosis of primary acute myelogenous leukemia blasts. *Leukemia.* 2003;17:1783–1793.

28. Spiekermann K, Biethahn S, Wilde S, et al. Constitutive activation of STAT transcription factors in acute myelogenous leukemia. *European journal of haematology.* 2001;67:63–71.

29. Birkenkamp KU, Geugien M, Schepers H, et al. Constitutive NF-kappaB DNA-binding activity in AML is frequently mediated by a Ras/PI3-K/PKB-dependent pathway. *Leukemia.* 2004;18:103–112.

30. Birkenkamp KU, Geugien M, Lemmink HH, et al. Regulation of constitutive STAT5 phosphorylation in acute myeloid leukemia blasts. *Leukemia.* 2001;15:1923–1931.

31. Cook AM, Li L, Ho Y, et al. Role of altered growth factor receptor-mediated JAK2 signaling in growth and maintenance of human acute myeloid leukemia stem cells. *Blood.* 2014;123:2826–2837.

32. Bardet V, Tamburini J, Ifrah N, et al. Single cell analysis of phosphoinositide 3-kinase/Akt and ERK activation in acute myeloid leukemia by flow cytometry. *Haematologica.* 2006;91:757–764.

33. Min YH, Eom JI, Cheong JW, et al. Constitutive phosphorylation of Akt/PKB protein in acute myeloid leukemia: its significance as a prognostic variable. *Leukemia.* 2003;17:995–997.

34. Ricciardi MR, McQueen T, Chism D, et al. Quantitative single cell determination of ERK phosphorylation and regulation in relapsed and refractory primary acute myeloid leukemia. *Leukemia.* 2005;19:1543–1549.

35. Kampen KR, Ter Elst A, Mahmud H, et al. Insights in dynamic kinome reprogramming as a consequence of MEK inhibition in MLL-rearranged AML. *Leukemia.* 2014;28:589–599.

36. Kotecha N, Flores NJ, Irish JM, et al. Single-cell profiling identifies aberrant STAT5 activation in myeloid malignancies with specific clinical and biologic correlates. *Cancer cell.* 2008;14:335–343.

37. Gaipa G, Bugarin C, Longoni D, et al. Aberrant GM-CSF signal transduction pathway in juvenile myelomonocytic leukemia assayed by flow cytometric intracellular STAT5 phosphorylation measurement. *Leukemia.* 2009;23:791–793.

38. Gallay N, Dos Santos C, Cuzin L, et al. The level of AKT phosphorylation on threonine 308 but not on serine 473 is associated with high-risk cytogenetics and predicts poor overall survival in acute myeloid leukaemia. *Leukemia.* 2009;23:1029–1038.

39. Arber DA, Orazi A, Hasserjian R, et al. The 2016 revision to the World Health Organization classification of myeloid neoplasms and acute leukemia. *Blood.* 2016;127:2391–2405.

40. Marcucci G, Haferlach T, Dohner H. Molecular genetics of adult acute myeloid leukemia: prognostic and therapeutic implications. *J Clin Oncol.* 2011;29:475–486.

41. Papaemmanuil E, Gerstung M, Bullinger L, et al. Genomic Classification and Prognosis in Acute Myeloid Leukemia. *N Engl J Med.* 2016;374:2209–2221.

42. Ossenkoppele GJ, Janssen JJ, van de Loosdrecht AA. Risk factors for relapse after allogeneic transplantation in acute myeloid leukemia. *Haematologica.* 2016;101:20–25.

43. Rollig C, Bornhauser M, Thiede C, et al. Long-term prognosis of acute myeloid leukemia according to the new genetic risk classification of the European LeukemiaNet recommendations: evaluation of the proposed reporting system. *J Clin Oncol.* 2011;29:2758–2765.

44. Knight ZA, Lin H, Shokat KM. Targeting the cancer kinome through polypharmacology. *Nat Rev Cancer.* 2010;10:130–137.

45. Ciallella JR, Reaume AG. In vivo phenotypic screening: clinical proof of concept for a drug repositioning approach. *Drug Discov Today Technol.* 2017;23:45–52.

46. Zheng W, Thorne N, McKew JC. Phenotypic screens as a renewed approach for drug discovery. *Drug Discov Today.* 2013;18:1067–1073.

47. Irish JM, Hovland R, Krutzik PO, et al. Single cell profiling of potentiated phospho-protein networks in cancer cells. *Cell.* 2004;118:217–228.

48. Crowson CS, Atkinson EJ, Therneau TM. Assessing calibration of prognostic risk scores. *Stat Methods Med Res.* 2016;25:1692–1706.

49. Fine JM, Gray RJ. Proportional hazards model for the subdistribution of a competing risk. *J Am Stat Assoc.* 1999;94:496–509.

50. Heinzl H, Kaider A, Zlabinger G. Assessing interactions of binary time-dependent covariates with time in cox proportional hazards regression models using cubic spline functions. *Stat Med.* 1996;15:2589–2601.